Conduction states in oxide perovskites: Three manifestations of Ti^{3+} Jahn-Teller polarons in barium titanate

S. Lenjer, O. F. Schirmer, and H. Hesse
Fachbereich Physik, Universität Osnabrück, Osnabrück, Germany

Th. W. Kool
Laboratory for Physical Chemistry, University of Amsterdam, Amsterdam, The Netherlands
(Received 2 April 2002; published 7 October 2002)

A comprehensive study of conduction polarons in purified $BaTiO_3$ crystals, containing about 100-ppm Nb as extrinsic ions, is presented. Nb^{5+} is compensated by Ti^{3+} $(3d^1)$ ions, many of them isolated. Small Ti^{3+} polarons, stabilized by crystal strains, and polarons of intermediate size in less strained crystal regions are identified. Both species break the point symmetry, indicating stabilization by a tetragonal $T_2 \times e$ Jahn-Teller distortion. There is indirect evidence for the presence of bipolarons in the crystal ground state. They have a rather small dissociation energy, 0.01 eV. The investigations are based on electron paramagnetic resonance (EPR) performed at $T < 20$ K under application of uniaxial stress. This allows to obtain local information on the intrinsic Jahn-Teller properties of the conduction states of an oxide perovskite. For the small polarons stress has the following effects: (i) aligns the tetragonal Jahn-Teller axes along the stress direction, and (ii) enlarges the radius of the aligned orbitals, transforming them into intermediate ones. The stress alignment of the intermediate polarons is different: The Jahn-Teller axes orient perpendicular to the stress axis. Several of the polaron features are elucidated by comparison with the stress-dependent Jahn-Teller properties of the impurity ion Mo^{5+} $(4d^1)$, where the d electron is prevented from tunneling to its Ti^{4+} neighbors. The EPR of Ti^{3+} in reduced $BaTiO_3$ is attributed to polarons bound to doubly filled oxygen vacancies.

DOI: 10.1103/PhysRevB.66.165106 PACS number(s): 71.38.−k, 71.20.Ps, 76.30.Fc, 77.84.Dy

I. INTRODUCTION

The structure of conduction-electron states in oxide perovskites and especially in $BaTiO_3$ (BT) has been studied intensively in the past.[1–6] There is evidence that in this compound such carriers are on the verge of forming small polarons, i.e., the electrons are self-localizing within about one bond length. These previous studies, however, have been performed with strongly perturbed specimens, i.e., reduced ceramics or single crystals, containing intended or accidental defects. The corresponding spatially fluctuating potentials tend to induce the formation of small polarons, and conclusions from such investigations are not necessarily representative for unperturbed crystals. In this paper, in contrast, specially prepared specimens of high quality will be investigated, approaching the ideal case of no perturbation, thus furnishing information on the intrinsic nature of electron polarons in BT.

The present study is part of a systematic effort to elucidate the structure and further properties of polarons in oxide materials by electron paramagnetic resonance (EPR).[7] Such investigations, yielding the most detailed conceivable insight into the microscopic properties of such systems, establish a firm basis onto which interpretations of further, less conclusive experiments on global properties, such as optical absorption or conductivity, can be based. Using nearly ideal material, we succeeded in identifying the EPR of Ti^{3+} free polarons in an oxide perovskite, allowing to elucidate the intrinsic nature of such charge carriers. In the previously investigated strongly perturbed samples they are usually bound to defects at the low temperatures needed for EPR studies. Important structural information on the polarons is gained by observing the behavior of the EPR signals under uniaxial stress. It turns out that a Jahn-Teller (JT) effect (JTE) is at least partly responsible for the polaron formation. The specific nature of the Ti^{3+} $(3d^1)$ electron polarons is highlighted by comparing their stress dependence with that of a $(4d^1)$ electron, realized by a Mo^{5+} impurity in $BaTiO_3$. This system is quite similar to Ti^{3+}; both cases are distinguishable, however, with respect to the nature of their neighbors: Ti^{3+} is surrounded by ions of the same type, Ti^{4+}, whereas these ions differ from Mo^{5+}. Therefore a Ti^{3+} conduction electron has a strong tendency to be delocalized to its Ti^{4+} neighbors; this is absent for a d electron at a deep defect, such as Mo^{5+}.

In the first section a short overview on the general features of polarons and their connection with the JTE will be given. Then the experimental details of the investigation will be outlined. The experimental results follow then, starting with those referring to Mo^{5+}, succeeded by the Ti^{3+} features. A separate section is reserved for polarons bound to an oxygen vacancy in reduced BT. Each of these subsections will contain a specific discussion, dealing with the locally appearing results. A general discussion, including the comparison with a theoretical treatment of the structure of Ti^{3+} polarons in BT, follows and a summary will conclude the paper. Some of the main results of the EPR investigation of Ti^{3+} polarons have been published earlier in a very abridged way.[8] Here we present an extended treatment of the subject.

II. POLARONS

On general features of polarons recent overviews, e.g., by Emin and Holstein,[9] Devreese,[10] and Shluger and

Stoneham,[11] may be consulted. The latter paper is concerned especially with small polarons. The following brief introduction to the topic is centered on the symmetry aspects of polarons.

In crystalline matter conduction electrons can choose among equivalent sites. The dynamics of the carrier transport is determined by an interplay between interactions breaking the translation symmetry and those conserving it. Tunneling interaction, leading to band formation, belongs to the latter category. If it prevails, conserved translational symmetry is found, characterized by the same probability density of the charge carrier at each of the equivalent sites. A polarization of the lattice by the electron tends to decrease its mobility, up to the point where self-localization takes place, spontaneously breaking the translation symmetry of a system.

For small polarons the charge carrier and its accompanying lattice distortion are limited to about one lattice site and its first neighbors. Such polarons can form if the coupling to the lattice includes short-range contributions (see, e.g., Ref. 9). In all practical cases the transport of small polarons is characterized by thermally activated hopping, an incoherent process. Their tunneling can be neglected and they thus show broken symmetry. Large polarons, favored by long-range Coulomb interaction, can be considered to be the other boundary case. They extend beyond one bond length. Their transport occurs coherently and they thus conserve translational symmetry. Here the coupling to the lattice expresses itself, e.g., by renormalization of the carrier effective mass to its polaron mass.

Ideal polarons can be conceived theoretically; in real cases the interaction with lattice irregularities has to be taken into account. A major source of such perturbations are charge-compensating ions: one cannot dope a crystal to be *n*-conducting without introducing the corresponding donor cores. The best for which one can hope is to study the properties of polarons by approaching a situation of zero doping. Also crystal strains, caused by other sources, have to be considered. It is thus difficult to strictly separate the cases of spontaneous symmetry breaking from those where localization is biased by potential fluctuations.

The formation of polarons shows features similar to those met in the JT effect.[12] The latter applies to impurity ions exhibiting—in the case of unbroken point symmetry—orbital degeneracy or near-degeneracy of their ground states. Interaction with the lattice tends to break the point symmetry—leading to a static JT effect—because the resulting lifting of the degeneracy can lower the energy of the system. Still also JT cases of conserved point symmetry are encountered; these are the situations labeled dynamic JT effects. In these instances the renormalization of expectation values, for instance, of operators which restore the point symmetry, such as spin-orbit coupling, is described by the Ham reduction factors,[12] their inverses are analogs of the renormalized mass of large polarons. Static JT effects have features similar to those of small polarons. Also in the case of the JTE lattice strains play an important role. However, their influence is most pronounced for $E\times e$ situations, less for the $T_2\times e$ case, with which we deal in this paper. Depending on the relative influence of tunneling and strains, all cases starting from the purely dynamical case, where tunneling prevails, over quasidynamic, with little strains, to quasistatic, where some tunneling effects are still observable, up to the pure static situation have been classified and observed.[13]

A combination of JT and polaron features is found in JT polarons: They can form, if a mobile charge carrier finds degenerate orbital ground states at each of the equivalent sites of a crystal. In the special case treated here, Ti^{3+} $(3d^1)$ in the cubic symmetry of the *B* site of an ABO_3 perovskite, a threefold orbitally degenerate ground state is present in the initial, undistorted nearly octahedral crystal environment, the symmetry of the *d* orbitals symbolized by *xy*, *yz*, and *zx*. This degeneracy is spontaneously lifted by a tetragonal distortion, leading to a new, nondegenerate ground state, having *xy* symmetry, if the distortion axis is labeled *z*. It should be understood that each of the other tetragonal directions, *x* or *y*, can likewise be axes of equivalent distortions; the corresponding JT ground states have then *yz* or *xz* symmetry, respectively. Further details will be given in a later section. Such a JT effect can occur for the conduction electron at each of the Ti sites, breaking not only the local point symmetry but simultaneously also the translational symmetry. The concept of JT polarons[14] was a heuristic principle in the search for high-temperature superconductivity.[15] For present notions about the role of JT polarons in this field, see Müller (Refs. 16 and 17). Also several features of the colossal magnetic resistance compounds of the type $La_{1-x}Sr_xMnO_3$ originate from JT polarons, see, e.g., Ref. 18.

The combined interaction of two like charge carriers with the lattice can lead to a stabilization energy which is larger than that of two separate polarons. If this surplus binding energy of two carriers is larger than their Coulomb repulsion, they will attract each other, forming bipolarons. Unfortunately, in all practical cases approached so far by EPR (Ref. 7) studies, such bipolarons have been found to pair diamagnetically and thus to be EPR silent. Still their presence can be inferred sometimes in indirect ways.

III. EXPERIMENTAL DETAILS

The BT crystals used in our study were grown using the crystal vibration method[19] from a melt strongly deriched from the frequently present alkali acceptor impurities, such as Na or K. Such defects are usually compensated by oxygen vacancies, which are potential trapping centers for conduction electrons. The alkali ions were washed out from the starting component $BaCO_3$. Also the TiO_2 component was produced essentially free of alkali ions and likewise of Fe and Al by employing a special purification procedure. The presence of a small concentration of Nb as a background impurity, however, could not be prevented. The BT starting material and the crystals grown from it thus are weakly doped with Nb^{5+}. As quoted by the supplier of the TiO_2 component, the Nb content is about 150 ppm. Since the distribution coefficient[4] of Nb in BT is about 1, the Nb content in the grown BT crystals can be estimated to be around 100 ppm. In BT, Nb^{5+} acts as a donor and is compensated by Ti^{3+}. These ions lead to a bluish coloration of the crystals, which—in contrast to reduced crystals—cannot be removed

by oxidation. With crystals prepared in this way the EPR of isolated Ti^{3+} was observed[20] without further treatment. Resonances from reduced crystals or those grown from more impure starting materials are different. In addition to isolated Ti^{3+} also Ti^{3+}-Nb^{5+} pairs were identified. Astonishingly, a sizeable concentration of the Ti^{3+} ions is not associated with Nb^{5+} donors;[20] mainly these isolated Ti^{3+} ions are treated in this paper. The crystal containing Mo^{5+} was kindly made available by Dr. R. N. Schwartz, Malibu, California.

The EPR experiments were performed with a Bruker ER 200 S-SRC spectrometer near 9 GHz at temperatures between 4.2 and 20 K, achieved by an Oxford ESR 910 cryostat. Uniaxial stress was applied to the specimens using a setup as described by Kool.[21] In this context it is useful to mention that all the stress-induced phenomena reported in this paper take place in a completely reversible way without any hysteresis phenomena. Thus no stress-induced defect formation or other deterioration of the investigated samples occur.

IV. INTRODUCTORY EXAMPLE: JT EFFECT OF MO^{5+} IN BT

Figure 1 shows the angular dependence of the EPR spectra of Mo^{5+} ($4d^1$) in BT (Ref. 22) at 15 K for a rotation of the magnetic field in a (100) crystal plane. The branches in Fig. 1 result from the ^{96}Mo isotope, which has zero nuclear spin ($I=0$). The resonances of the remaining stable isotopes, having $I\neq 0$, show hyperfine structure,[22] which supports the assignment to Mo but is not relevant in the present context. The lines in Fig. 1 mark the resonance positions predicted by the spin Hamiltonian $H=\mu_B \mathbf{BgS}$ with $S=\frac{1}{2}$; the principal values of the nearly axial g tensor, typical for Mo^{5+}, are given in Table I. The evaluation indicates that the Mo^{5+} ion resides in an almost perfect tetragonal environment, slightly trigonally distorted, as expected if it replaces Ti^{4+} in the rhombohedral crystal phase of BT, present below 183 K. Small tiltings of the g-tensor principal axes, consistent with the influence of the weak trigonal crystal-field component, cause the small splittings in Fig. 1.

The prevailing tetragonal symmetry is caused by a static $T_2\times e$ JT effect.[12] Here the representation symbol T_2 indicates the threefold degeneracy and the symmetry properties of the orbitals (xy, yz, zx), and e the distortion mode of the crystal environment (Fig. 2). The presence of a JT effect is proved by the behavior of the system under uniaxial stress, as applied along a [100]-type axis. In such an experiment the concentration of occupied d orbitals extending perpendicular to the stress axis increases, i.e., those of xy symmetry do, if stress is applied along a [100]-type direction called z—an assumption that will be made throughout this paper without limiting generality. The sample could only be rotated around the stress axis i.e., the magnetic field was always perpendicular to this axis and thus varying in the xy plane. The xy orbitals then lead to the nearly-angle-independent branch in Fig. 1. Simultaneously the orbitals extending along the stress axis, i.e., those of xz and yz types, are depopulated. The orbital occupation changes are caused by a reorientation of the tetragonal axes, and the electrons—previously equally distributed over the three possible distorted configurations—now favor that orbital having the lowest energy in the stressed case. The rearrangement of the electrons to the new energetical situation takes place at small stresses already and at temperatures as low as 4.2 K.

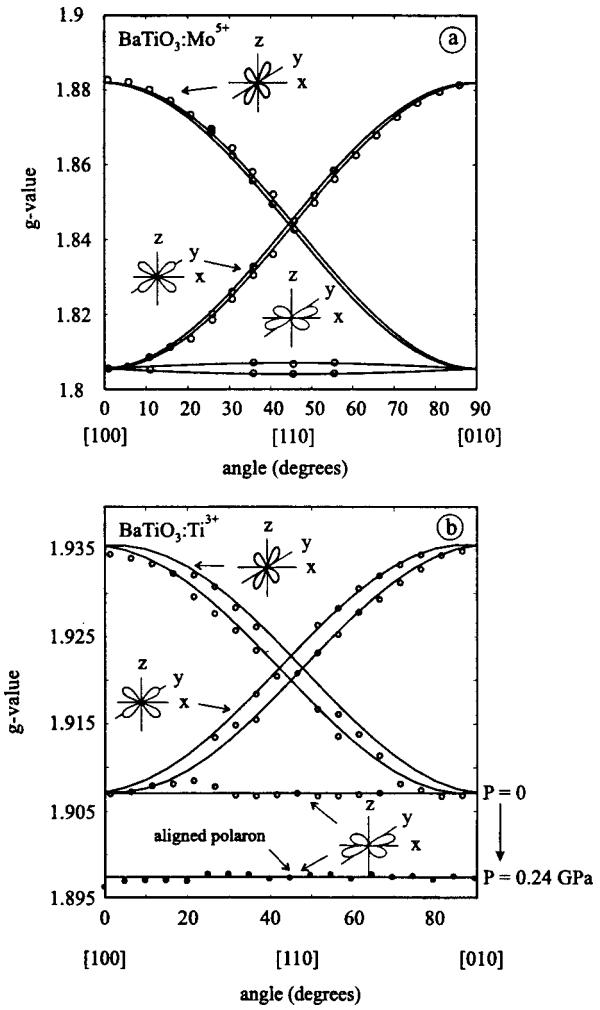

FIG. 1. (a) The g values of the paramagnetic resonances of Mo^{5+} in BT depending on the angle between crystal axes and direction of magnetic field. The lines are the resonance positions calculated on the basis of the g-tensor information given in Table I. The small splittings are caused by the weak trigonal crystal-field component of the rhombohedral phase of BT. The orbitals corresponding to the various branches are indicated. Under uniaxial stress, assumed to be applied along the [001] axis, the intensity of the lowest, nearly-angle-independent branch increases at the expense of the upper two branches. (b) Same for the Ti^{3+} small polaron signals. Under uniaxial stress, alignment occurs, as for Mo^{5+}. In addition the lowest branch shifts to lower g values, as indicated.

We want to mention here that also the weak trigonal crystal-field component will lift the assumed degeneracy of the T_2 orbitals into a singlet and a doublet. This splitting, however, is expected to be small enough that it can be overridden by the tetragonal JT coupling. But still in the strict sense one ought to speak rather of a pseudo-JTE, taking into account the slight initial lifting of the degeneracy, instead of a pure JTE.

TABLE I. Principal g values of the various Ti^{3+} polaron manifestations and related defects.

	$B\|\|x$	$B\|\|y$	$B\|\|z$
Ti^{3+} (small polaron)			
$P=0$	1.907[a]	1.907	1.936[a]
$P=0.24$ GPa	1.898[a]	1.898	aligned[b]
Ti^{3+}-Nb^{5+}[b]	1.892	1.892	1.932
Ti^{3+} (intermediate polaron)			
$P=0$	1.890	1.890	1.928
$P=0.24$ GPa	1.897	1.935	aligned[b]
Mo^{5+}	1.806[a]	1.806	1.882[a]
Axial Ti^{3+} centers in reduced $BaTiO_3$	1.920	1.920	1.937
	1.916	1.916	1.930
	1.911	1.911	1.930

[a]The relevant axes are slightly tilted in a (110)-type plane towards [111] by 0.9° for Mo^{5+} and 4.1° for Ti^{3+}. The branches in Fig. 1 mark the resonances resulting from all equivalent centers possible in cubic symmetry.

[b]"Aligned" means that under stress only one axis, z, is realized. A measurement for **B** along the stress axis is not possible.

As an alternative to the $T_2\times e$ JTE the association of Mo^{5+} with an ionic defect could cause the tetragonal symmetry. This, however, would not be consistent with the observations. The rearrangement of a JT distorted environment of Mo^{5+} during reorientation involves only slight shifts of the relevant ions, whereas a defect next to Mo^{5+} would have to change sites. In the latter case the reorientation barrier therefore is expected to be much higher than in the previous one. For instance, Hackmann and Kanert[23] found for the hopping time τ of an oxygen vacancy between oxygen sites in $SrTiO_3$ the temperature dependence $\tau=\tau_0\exp(0.62\ \mathrm{eV/kT})$, with $\tau_0=5.3\times10^{-14}$ s, yielding $\tau=450$ h at 600 K. At 4.2 K the corresponding time would be effectively infinite. Taking such an oxygen vacancy as a sample case for an associated ionic defect in the present case, no movement would be expected at 4.2 K, the temperature at which reorientation was observed. If instead of a vacancy an extrinsic defect was associated with Mo^{5+}, the barrier for reorientation would even be higher, because then two ions would have to exchange sites.

In the absence of external stress the JT ground states, resulting from equivalent [100]-type lattice distortions, have equal energy. This is necessarily so because the JT coupling is an internal interaction, which cannot lift the equivalence of the three tetragonal lattice rearrangements. External stress, on the other hand, favors one of the JT ground states with respect to the other two. The orbital population is determined by the Boltzmann distribution. Quantitatively, this leads to[21]

$$\frac{2I_{\mathrm{al}}}{I_{\mathrm{nal}}}=\exp\left(\frac{-\Delta E}{kT}\right)$$

with

$$\Delta E=\frac{3}{2}\frac{V}{c_{11}-c_{22}}P \qquad (1)$$

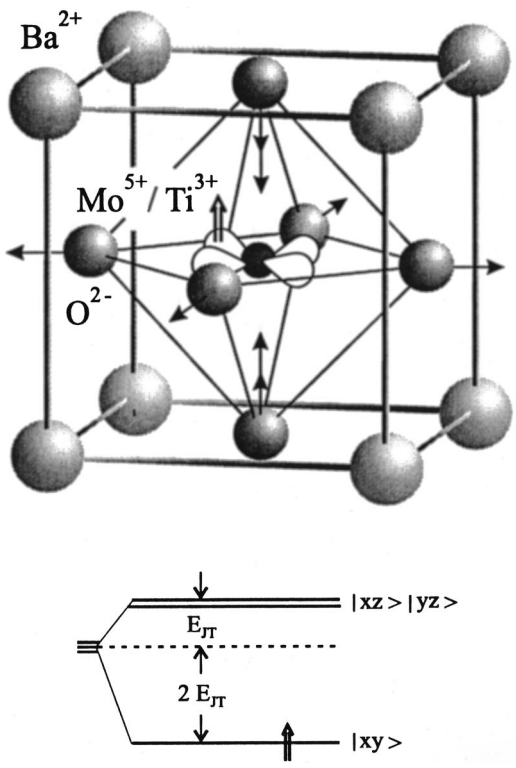

FIG. 2. Static $T_2\times e$ Jahn-Teller effect of (nd^1) ions in the octahedral crystal field of a perovskite unit cell. One of the three equivalent JT distortions is indicated. The indicated orbital ground state is of xy type. In the lower part it is shown how the electron energy is stabilized by $-2E_{\mathrm{JT}}$ by this distortion. Since simultaneously the elastic energy rises by E_{JT} a total stabilization by $-E_{\mathrm{JT}}$ results.

with I_{al}: EPR signals of aligned (xy-type) centers; I_{nal}: EPR signals of not aligned (xz, yz) centers; P: stress; V: stress-coupling coefficient; and c_{ii}: relevant stiffness constants of BT. Figure 3 shows the experimentally determined quantity $\ln(2I_{\mathrm{al}}/I_{\mathrm{nal}})$ as depending on P. Using the stiffness parameters[24] $c_{11}-c_{22}=66$ GPa the value of $V=0.90\times10^4\ \mathrm{cm}^{-1}$ is derived. The fact that xy orbitals are stabilized by stress along z is consistent with the corresponding slight deformation of the octahedron surrounding Mo^{5+}: The axial oxygen ions along the stress axis will approach Mo^{5+}, whereas the equatorial ones will move somewhat outside. The negative charge distribution in the xy orbital then avoids the ligands more than in xz or yz.

In contrast to the situation of Ti^{3+}, to be treated in the next section, no stress-induced changes of the Zeeman or hyperfine splitting of the aligned orbital, xy, were observed. This means that the radial extension of the orbital is not altered.

V. EPR STUDIES OF Ti^{3+}

A. Small polarons

The EPR signals in Fig. 4 have first been attributed to isolated Ti^{3+} and Ti^{3+}-Nb^{5+} by Possenriede *et al.*[20] The assignment of the latter resonances is based on the ten-line

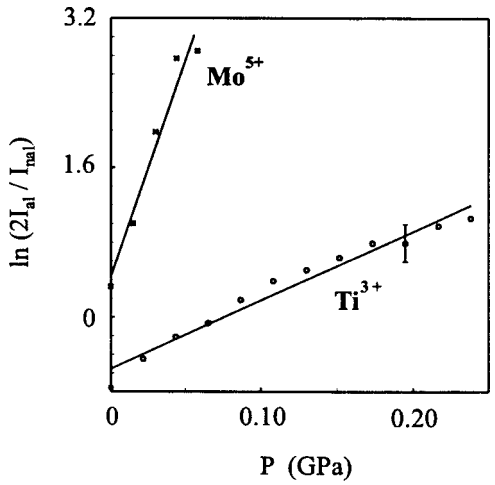

FIG. 3. Stress alignment of the three equivalent JT ground states according to Eq. (1). The stress-coupling coefficients, corresponding to the slopes of the lines, are 0.90×10^4 cm^{-1} for Mo^{5+} and 0.27×10^4 cm^{-1} for Ti^{3+}. In strain-free crystals the lines should cross the ordinate at 0. The shown deviations are attributed to nonzero initial average strains.

hyperfine structure, typical for ^{93}Nb ($I=9/2$; 100% natural abundance). Although one would expect that a conduction electron has a lower energy at a Nb^{5+} site, one has to accept the experimental finding that the electron mainly resides at Ti, as implied by the notation Ti^{3+}-Nb^{5+}: (i) the g values (Table I) are nearly identical to those of isolated Ti^{3+}. Nb^{4+} in a sixfold cubic environment would lead to quite different g tensors.[25] (ii) The hyperfine splitting caused by ^{93}Nb is comparatively small.[25] The Nb donor thus forms a rather shallow potential. This is supported by the fact that a sizeable concentration of Ti^{3+} is isolated (Fig. 4). The spontaneous transfer of the Nb donor electron to the Ti conduction band in $BaTiO_3$ has recently been mentioned in Ref. 26. We are mainly concerned here with the properties of such isolated Ti^{3+}. In an environment of equivalent Ti^{4+} ions they indicate broken translational symmetry, typical for small polarons. Without application of external stress, the EPR of isolated Ti^{3+} (Fig. 4) shows features similar to those of Mo^{5+}; the topology of Fig. 1(b) is isomorphous to that of Fig. 1(a) again indicating nearly exact tetragonal symmetry.

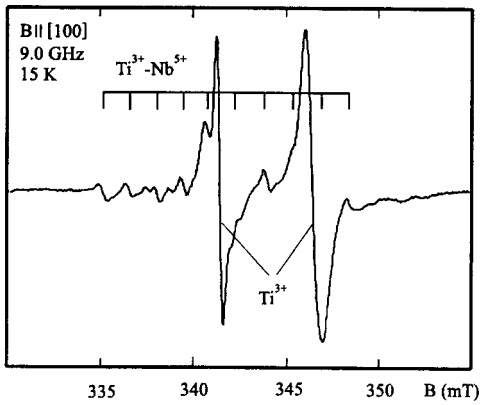

FIG. 4. EPR signals of Ti^{3+} and Ti^{3+}-Nb^{5+} in BT at 15 K.

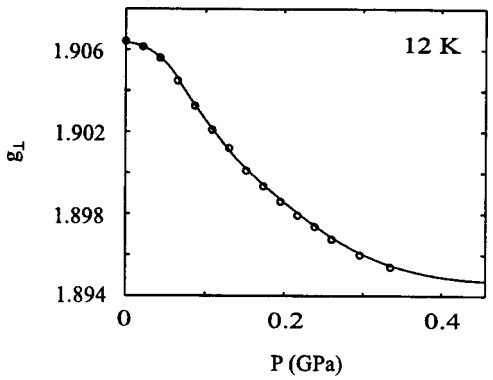

FIG. 5. Change of the $g_\perp$ value of the Ti^{3+} small polaron signal depending on stress. The line is a guide for the eye.

Information on the g tensors is given in Table I. Also a stress-induced alignment occurs, quite comparable to the case of Mo^{5+}. This again proves the presence of a JT effect. The stress-coupling factor, however, is much smaller than in the previous case (Fig. 3). Also in strong contrast to the situation of Mo^{5+} the $g_\perp$ value of the aligned xy orbital decreases strongly when P is raised [Figs. 1(b) and 5].

No change of the EPR spectra occurs for stress along the trigonal [111]-type directions. Since the JT distortions create tetragonal symmetry along the three [100]-type directions, [111] stress affects all these distortions equally, and none of the JT ground states is preferred energetically with respect to the other two. Also this demonstrates that the slight trigonal crystal-field component at the Ti sites, present in the low-temperature rhombohedral crystal structure, does not have to be considered in our argumentations.

What causes the stress-induced line shift [Figs. 1(b) and 5], present for Ti^{3+} but not for Mo^{5+}? The $g_\parallel$ and $g_\perp$ values of an (nd^1) ion in axial symmetry with an xy lowest orbital are given by[27]

$$g_\parallel = g_e - \frac{8k\lambda}{E_\parallel}$$

and

$$g_\perp = g_e - \frac{2k\lambda}{E_\perp}. \qquad (2)$$

Here the deviations from the free spin value g_e are caused by spin-orbit admixture λ of excited orbitals, competing with the crystal-field excitations $E_\parallel$ and $E_\perp$. We cannot measure $g_\parallel$ of the aligned xy state under stress, because the direction of the latter, which defines the tetragonal axis, always lies perpendicular to **B**. $E_\perp$ is caused by the JT splitting, separating the xz and yz orbitals from the xy ground state, Fig. 2. The reduction factor k comprises two components: $k = k_{cov}k_{JT}$, where the first one takes into account covalency,[27] and the second, quenching of orbital angular momentum by the JT effect.[27] Since $\lambda>0$ for Ti^{3+}, a decrease of $g_\perp$ is caused by a declining $E_\perp$. In the case of a ($T_2\times e$) JTE the energy spacing $E_\perp$ corresponds to $3E_{JT}$ (Fig. 2); we thus conclude that E_{JT} is decreasing. The influence of k_{JT} works

into the same direction:[12] $k_{JT}=\exp(-3E_{JT}/\hbar\omega)$; here $\hbar\omega$ is the energy of the representative coupling vibration.

We shall attribute the change of E_{JT} to an increasing delocalization of the polaron wave function under rising stress. This is suggested by the observation that there is no stress-induced g shift for Mo^{5+}, which does not have the banding tendency of Ti^{3+}. In order to show that delocalization tends to decrease the JT coupling[28] we point out that the JT energy can be written as a sum of contributions resulting from the JT coupling to phonons specified by different wave vectors q: $E_{JT}=\Sigma_q E_{JT}^q$. If the extension of a polaron wave function, labeled a, exceeds the wavelength $2\pi/q$ of a coupling phonon, the interaction with such a phonon is averaged away and thus the corresponding E_{JT}^q decreases with rising polaron extension. Quantitatively,[28]

$$E_{JT}^{\mathbf{q}}\propto\int e^{i\mathbf{qr}}|\Psi(\mathbf{r})|^2 d\mathbf{r}=\frac{1}{\left(1+\frac{1}{2}a^2q^2\right)^2}, \tag{3}$$

assuming, as a model case, a $1s$ hydrogenic $|\Psi(\mathbf{r})|^2$ with radius a. It is seen that with rising polaron radius a, phonons with large q are progressively excluded from the coupling. Consequently, E_{JT} is lowered if the polaron radius increases.

Why is the radius of the xy ground state of the polaron increased under stress? The following model may be put forward. Each of the Ti^{3+} ions is accompanied by a JT distortion; in the unstressed crystal all three distortion axes are present with a statistical weight of $\frac{1}{3}$. The resulting disorder will lead to sizeable local potential fluctuations to which each Ti^{3+} contributes as well as adjusts itself in a self-consistent way. To this disorder caused by the small Ti^{3+} polarons discussed here there will be additional contributions by the further Ti^{3+} objects introduced below. The potential fluctuations resulting from these sources will tend to decrease the mobility of the conduction electrons, thus lead to enhanced coupling to the lattice, and correspondingly lower the wave-function radius. If the disorder is removed by stress alignment of the JT axes, the potential fluctuations become weaker, and delocalization sets in, causing a lower E_{JT}. This chain of arguments is supported by the fact that there are no stress-dependent g shifts for Mo^{5+}: because of the inequivalence of Mo^{5+} to its Ti neighbors, the radius of the Mo^{5+} ground state is expected to be smaller from the outset and not to be increased by stress. The situation can also be described in the following way: Under increasing alignment the crystal becomes more strain-free and the orbital approaches the eigenstate expected for a conduction electron in an ideal BT crystal. Such states are predicted to be of intermediate size by an embedded-cluster calculation,[29] to be commented below. Small polarons can form only if supported by lattice irregularities, such as strains. As a corollary we furthermore arrive at the important conclusion that the $g_\perp$ value of Ti^{3+} gives an indication for the radius of the ground-state orbital.

B. Intermediate polarons

All the EPR studies of Ti^{3+} reported so far (Fig. 4) have been performed at 16 K, because this allowed to observe the respective signals essentially unperturbed by other ones appearing only at low temperatures (Fig. 6). Furthermore, quite unexpectedly, the EPR intensity of the Ti^{3+} polarons rises with temperature (Fig. 7). This increase of the small polaron intensity I occurs exponentially according to the relation

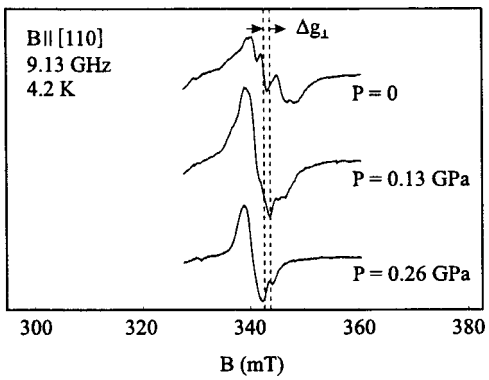

FIG. 6. EPR signals of the investigated crystal at low temperature (4.2 K) for various stresses. The small polaron resonances and their shift under stress [see Figs. 1(b) and 5] are indicated by the vertical dashed lines, marking the initial ($P=0$) and final ($P=0.26$ GPa) positions. They are seen to be superimposed upon a strong resonance signal, which is attributed to polarons of intermediate size. The width of this signal is larger than that of the small polarons and decreases with rising stress (see also Fig. 8 below). The intensity of the small polaron signals decreases under stress [see also Fig. 11(a) below].

$$I=\frac{a}{T}\exp\left(\frac{-E_a}{kT}\right)+c. \tag{4}$$

The factor $1/T$ takes account of the Boltzmann distribution between the EPR Zeeman levels. This influence, on the basis of which the usual increase of EPR signals with lowering temperature is expected, is overcompensated by the exponential. With $E_a=0.01$ eV it appears to describe the activation of the Ti^{3+} small polaron EPR from a diamagnetic precursor state. The parameter c denotes a temperature-independent background concentration.

At low temperatures (e.g., at 4.2 K in Fig. 6) the EPR spectra of the material are dominated by a broad structure,

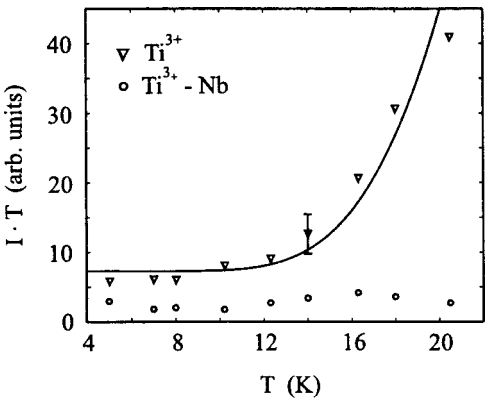

FIG. 7. Increase of the small polaron signal with temperature. The line is calculated on the basis of Eq. (4)

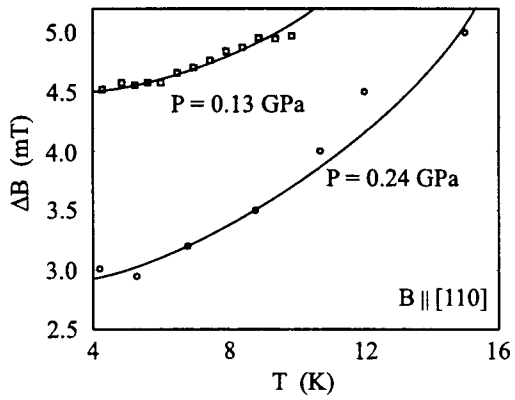

FIG. 8. Dependence of the width of the intermediate polaron signals in Fig. 6 on stress and temperature: the widths of the lines decrease with rising stress and they increase with rising temperature. The lines are guides for the eye.

attributed to Ti^{3+} polarons of intermediate size for reasons to be discussed below. It is not observable at 16 K, because its width rises strongly with temperature (Fig. 8). The broad signal is seen to be composed of two angular-dependent components, if observed for clarity under $P=0.24$ GPa (Fig. 9). Using this stress leads to sharper component lines, as indicated in Figs. 6 and 8, and thus allows a more definite signal decomposition. But also for $P=0$, where the width is large (at least 7 mT), an analysis has been attempted and—despite limited resolution—it was clearly observed that in this case an additional, third component contributes to the spectra (Fig. 9). In this figure the $P=0$ data are compared to those taken with $P=0.24$ GPa. All the relevant *g*-tensor components are listed in Table I. It is seen (Fig. 9) that for $P=0$ the responsible centers are characterized by three equivalent tetragonal axes. For $P=0.24$ GPa the horizontal branch does not appear any more, indicating a stress-induced alignment of the axes. It is thus again straightforward to assume a JT effect as the cause of the tetragonality. However, in contrast to the previous case of the small Ti^{3+} polarons, here the branch corresponding to orbitals extending perpendicular to the stress axis (i.e., of extended *xy* type) is removed under stress. The alignment thus rather occurs as sketched in Fig. 10, favoring extended orbitals of *yz* and *xz* types.

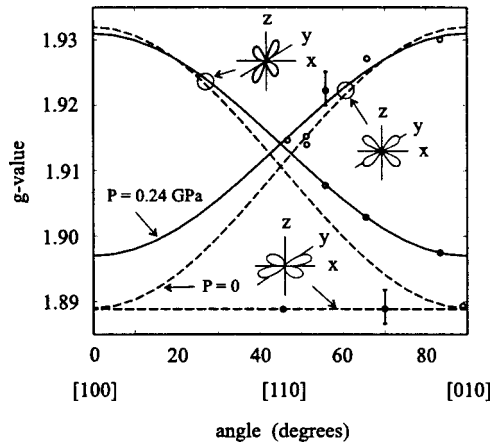

FIG. 9. Angular dependence of the intermediate polaron resonances under $P=0$ (full lines) and $P=0.24$ GPa (dashed lines).

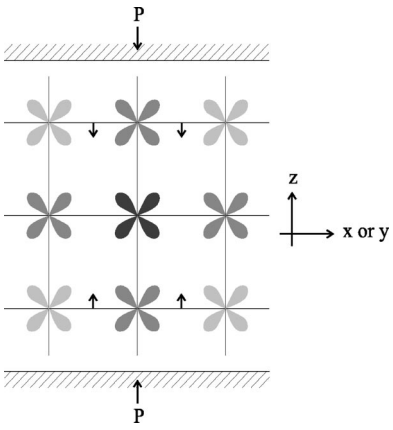

FIG. 10. Scheme of the alignment of the plane of the intermediate polaron orbitals under stress as applied along the indicated direction. The shown delocalization of the electron density is based on the calculations in Ref. 29. The shadings represent the electron densities at the respective sites.

There is no doubt that the new centers also have to be attributed to Ti^{3+}: (i) Especially their *g* values are quite close to those of the small Ti^{3+} polarons under stress. (ii) On the other hand, they are distinctly different from those of other defect species, such as Mo^{5+} (Table I). As mentioned above, the smaller *g* values of the present Ti^{3+} signals point to a larger polaron extension. Not knowing the radii of the corresponding wave functions exactly, we cautiously label them intermediate polarons, leaving open the question of whether they can already be considered large ones. As seen, e.g., in Fig. 6, they coexist with the small polarons and can be assumed to exist in crystal regions that are more strain-free from the beginning.

It should be noted that the EPR signals of the intermediate polarons and especially their large widths correspond to a much larger concentration, if compared to the small ones. By calibration with an EPR standard it is found that the small polaron concentration is about 0.1 ppm (as related to the Ti content) at 14 K, whereas the intermediate ones are present with about 4 ppm. Thus most of the paramagnetic Ti polarons manifest themselves as intermediate ones. The majority of Ti^{3+} ions, however, must be present in a diamagnetic configuration, since the concentration of Nb^{5+}, to be compensated, is of the order of 100 ppm, see above. This additional reservoir of Ti^{3+} is likely to consist of bipolarons, as outlined below.

First the remarkably different stress alignment of the intermediate polarons will be discussed. As pointed out, their energy is determined less by the JT coupling to the lattice and more by the onset of banding, i.e., by a decrease of kinetic energy accompanying delocalization. All orbital configurations tending to increase the banding thus will be stabilized. Under stress the crystal will expand slightly perpendicular to the stress axis; a dilatation by about 3×10^{-3} per 1 GPa is calculated from the elastic parameters of BT.[24] There will thus be a limit for the stress-induced expansion of an *xy*-type orbital, since under increasing stress the Ti^{4+} neighbors along *x* and *y* will start to be removed from the initial

Ti^{3+} site and tunneling to the equatorial Ti^{4+} neighbors will therefore be limited. On the other hand, the Ti^{4+} neighbors along *z* will move closer to Ti^{3+} (Fig. 10); a compression by 12×10^{-3} per 1 GPa is calculated. Now a more efficient banding along this direction is possible, but only if the ground-state orbital of Ti^{3+} reorients in such a way as to move high density towards the *z* direction, i.e., leave the *xy* configuration and assume an *xz* or *yz* character, as shown in Fig. 10. This banding along the stress direction is mediated by the p_π orbitals of the O^{2-} ions between the Ti ions neighboring along the stress axis. The increase of banding under uniaxial stress is also suggested by the observation, that the shape of the EPR signal assigned to the intermediate polarons tends to become more Lorentzian with increasing stress, indicating an onset of exchange narrowing.

In the previous publication[8] on the topic a reorientation of the intermediate polarons, as presented here, was not taken into account as a possibility. The explanation of the angular dependence of these stress-aligned objects, different from those of the small polarons, was rather based on the assumption that the conduction band had a minimum at $k\neq0$. However, this model could not account for the fact that the *g* values of the intermediate polarons changed so little under stress $P\neq0$.

In this context two observations are mentioned that underline the present interpretation of the alignment of the intermediate polarons. In the tetragonal phase of BT, existing between 8 °C and 120 °C, the crystal is elongated along its fourfold, [001]-type axis. This corresponds to a negative stress, if compared to our present investigations. Assuming that the majority of the conduction electrons form intermediate polarons (or bipolarons, see below) such a negative stress will favor orbital expansion perpendicular to the elongated tetragonal axis. In this way it stabilizes the extended *xy*-type states. This explains the fact that the electrical conductivity in tetragonal BT is larger perpendicular to the tetragonal axis than parallel to it.[4] It should be noted that this feature cannot be explained by the alignment behavior of the small polarons: According to their alignment behavior, see above, negative stress should orient the plane of the corresponding orbitals along the axis, favoring conduction along and not perpendicular to it.

These arguments are furthermore supported by the fact that there are no indications for small or intermediate polarons in $SrTiO_3$, also slightly doped with Nb;[30] the material rather shows the behavior of free electrons moving in a wide band. This is due to the slightly shorter lattice constant of the material, about 2% less than that of BT 4.00 Å. Thus band transport is expected and found to be the prevailing transport mechanism in $SrTiO_3$. This may explain the circumstance that EPR of Ti^{3+} conduction states has never been observed in $SrTiO_3$. These findings show how sensitively the Ti^{3+} conduction states in Ti-oxide perovskites react to lattice changes. Also the different manifestations of the JT effects of Mo^{5+} in both compounds can be explained on this basis: while static in BT, they are dynamic in $SrTiO_3$.[31]

C. Bipolarons

As has been mentioned above, there is evidence that Ti^{3+} can manifest itself in a third way in BT. The temperature dependence of the small polaron Ti^{3+} concentration (Fig. 7) suggests that this object arises from a diamagnetic background with an activation energy of 0.01 eV. Since diamagnetism is typical for all bipolarons indirectly identified so far in the course of EPR studies,[7] it is likely that the observed Ti^{3+} signals arise from thermal dissociation of bipolarons, for which the energy gain via a common lattice distortion by two electrons outweighs their Coulomb repulsion by the very small amount of 0.01 eV. The recombination of dissociated electrons to bipolarons is expected to be strongly impeded by slow diffusion. Under this circumstance a background concentration of those Ti^{3+} polarons will thus remain which are kinetically hindered from recombination. This accounts for the parameter *c* in Eq. (4). The present findings support an earlier suggestion[32] that the ground state of conduction electrons in BT consists of bipolarons. Since the Ti^{3+} concentration in the crystals, which can be detected by EPR is only about 4 ppm (see above), whereas the total Nb^{5+} concentration is estimated to be about 100 ppm, it is likely that a sizeable concentration of Ti^{3+} bipolarons is present in the investigated specimens at low temperatures. The orbital structure of Ti^{3+} bipolarons is known from crystallographic studies of Ti_4O_7.[33] Here Ti^{3+}-Ti^{3+} pairs at neighboring sites have been identified. This is different from the electron distribution in bipolarons postulated previously by Moizhes and Suprun[32] for BT, assuming two electrons on one Ti site, equivalent to Ti^{2+}.

D. Further observations

In addition to the shift of their resonance positions, the small polarons also show a decline of their intensity [Fig. 11(a)] under increasing stress. Apparently this is caused by the transformation of these objects into polarons of intermediate size, as indicated in Fig. 11(b). Here it is seen that the concentration of small polarons relative to the intermediate ones decreases. It is also observed that the width of the EPR signals of the intermediate polarons declines under stress (Fig. 8) whereas that of the small polarons is rather insensitive to such influence. To explain this we have to consider first that the wave function of the small polarons has high amplitude near one Ti site only. Because of the low tunneling tendency of small polarons, their energy is dominated by the corresponding rather localized lattice distortion. The strain disorder in the unstressed crystal primarily serves to localize the charge carrier and contributes comparatively little to its energy. We therefore have a unique wave function for all small polarons and the EPR signals thus are rather sharp. In intermediate polarons, on the other hand, an electron encompasses several Ti ions, and the wave-function amplitudes at each of these sites are influenced by the combination of stronger tunneling, the remaining locally varying strains, and the weaker polaron coupling. Relative to it, the strain remnants now are more important. The wave function in this case is therefore not unique and varies from carrier to carrier, depending on the local strains. Therefore also the *g* values, via the level energies [Eq. (2)] depending on the wave functions, are expected to have larger spreads. The stress alignment on the other hand sorts out definite distortions, overrid-

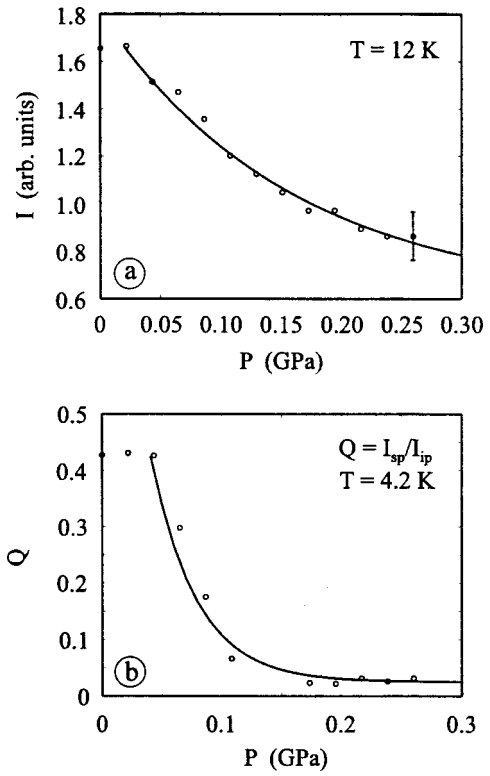

FIG. 11. (a) Decrease of the intensity I_{sp} of the small polaron signals under rising stress. The line is a guide for the eye. (b) Decrease of the intensity I_{sp} of the small polaron signals relative to those of the intermediate polarons I_{ip}, under rising stress. The line is a guide for the eye.

ing the internal strains, and thus leads to more defined and equal wave functions. A line narrowing results. Such an effect has previously been reported for the stress dependence of magnetic-resonance linewidths of a defect in silicon;[34] in this specific case a carrier could choose among three sites equivalent with respect to the defect core, and tunneling was competing with strains, as in the present case. A pronounced EPR line narrowing was observed under stress.[34]

On the same basis the width of the intermediate polarons, rising with temperature, Fig. 8, can be explained. Because of the increased tunneling the mobility of the intermediate polarons is raised. The accompanying lattice rearrangements raise the probability for longitudinal T_1 relaxation of the spins, leading to increased linewidths.

VI. Ti^{3+} POLARONS BOUND TO AN OXYGEN VACANCY

Previously[35] several Ti^{3+} defects with g tensors slightly different from those of the Ti^{3+} small polaron were observed by EPR in undoped BT after a strong reduction treatment. Among them there are three axially symmetric ones (see Table I) having somewhat smaller $g_\perp$, i.e., slightly larger axial splitting energies [Eq. (2)] between the T_2 sublevels than the small polaron resonances. These signals have before[35] been assigned to the most fundamental intrinsic defects in BT, oxygen vacancies, V_O, i.e., to one electron captured at an empty oxygen site, leading to $V_O^\bullet$. Experimentally it was established that the ground-state wave functions were of T_2 (e.g., *xy*) type, similar to the case of the small polarons treated above. This electronic structure of the defect appeared to be in accord with a model derived from previous theoretical treatments of the $V_O^\bullet$ center;[36,37] they indicated the ground-state of the system to be of T_2 type. However, for several reasons, listed, for instance, in Ref. 38, these calculations did not model the situation reliably. More recent theoretical treatments,[38–40] using larger orbital basis sets than the previous ones, definitely and independently showed that the ground-state wave function of $V_O^\bullet$ rather has a $(3z^2-r^2)$ electronic structure and a high density within the vacancy. Centers with orbitals of this symmetry could, however, not yet be identified in reduced BT, although they would be easy to monitor by EPR.[41]

How can this discrepancy be resolved? The isolated vacancy does not appear in a paramagnetic state if it is a negative U system. This means[42] that two electrons in V_O do not repel ($U>0$) but attract each other by joint lattice distortion, outweighing the Coulomb repulsion. This leads to a diamagnetic ground-state, just as for bipolarons, which are special negative U systems referring to quasifree and not to bound charge carriers. For a "negative U"-V_O center only the configurations with no electrons $V_O^{\bullet\bullet}$ or with two electrons V_O^x are stable.[42] The nonexistence of the singly ionized oxygen vacancy $V_O^\bullet$—being paramagnetic—is possibly also supported by defect chemical studies of BT: under oxygen pressures between[43] 10^5 and 10^{-15} Pa there is no evidence for singly ionized oxygen vacancies $V_O^\bullet$, at equilibrium conditions. How are the Ti^{3+} EPR signals arising from reduced BT (Ref. 35) to be explained then? The charge states V_O^x and $V_O^{\bullet\bullet}$ have been identified by Müller, Berlinger, and Rubins[41] indirectly by their influence on the EPR of neighboring Ni^{3+} $(3d^7)$ impurity ions (Fig. 12) in $SrTiO_3$. Ni^{3+} has a strong crystal field, low spin configuration, i.e., the T_2 subshell is filled and the seventh electron is accommodated in an x^2-y^2 orbital, if V_O is saturated with two electrons. If it is empty, the $3z^2-r^2$ orbital is lowest (Fig. 12). No evidence was found for the configuration with one electron in V_O, supporting the negative U nature of V_O. Because the effect of the full V_O is evidently to repel negative charges at a neighboring cation, the lowest orbital of a Ti^{3+} ion next to full V_O is thus expected to be of *xy* type (Fig. 12), as established experimentally. This model, corresponding to a bound Ti^{3+} polaron next to a filled V_O, is able to explain the configuration of one of the axial Ti^{3+} centers in Table I. Because $\Delta g_\perp$ in this case is lower than for the small polaron, as can be seen from Table I, the axial field is stronger than in the latter case. Here the splitting of the T_2 states results not only from the JT-type stabilization of the *xy* orbital but also from the influence of the neighboring full V_O, evidently lowering the energy of this orbital and raising the energy of *xz* and *yz*.

Exactly one of the three axially symmetric centers, identified in reduced BT, as listed in Table I can then be assigned to a Ti^{3+} polaron bound next to V_O^x. It is not known which one this is. The other axial centers of this type as well as several other ones with nonaxial symmetry[35] are likely to arise from a Ti^{3+} polaron bound to V_O^x plus additional de-

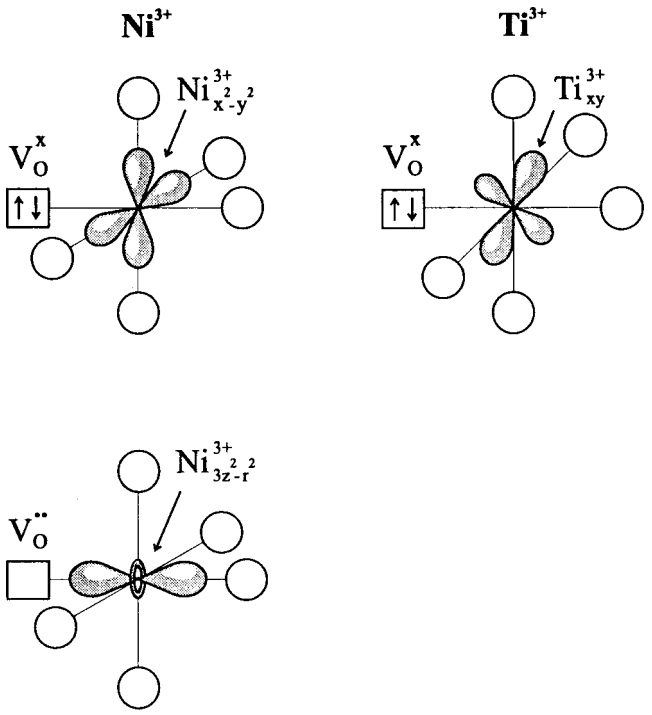

FIG. 12. Structure of the Ti^{3+} polaron bound to V_O^x as compared to established models of Ni^{3+} next to V_O; see Ref. 41.

fects. They are all characterized by smaller average $\Delta g_\perp$ values than for small polaron Ti^{3+}, supporting the association with defects. This occurs especially if the crystals contain acceptor ions, i.e., ions negatively charged with respect to the lattice. It is expected that in these cases Ti^{3+} is associated both with V_O and the acceptor, situated in different relative orientations. This has been proved[35] especially for associations with Na and K. Concluding, it appears that the Ti^{3+} EPR signals observed in reduced BT have to be attributed to a polaron bound to V_O^x, either isolated or in conjunction with a second lattice perturbation.

Such systems demonstrate the influence of defects on the polaronic properties of the material. This supports the remark, made in the introduction, that no information on the intrinsic properties of polarons is to be expected in reduced or strongly doped crystals. The localization by defects will prevent the formation of intermediate polarons.

VII. DISCUSSION

The theoretical studies mentioned above are based on an embedded-cluster modeling[29] of Ti^{3+} polarons in BT. These calculations clearly show that the eigenstate of a Ti^{3+} conduction electron in ideal BT is represented by a polaron of intermediate size. However, this occurs only if correlation effects are carefully taken into account.[38] Hartree-Fock-type approaches tend to predict too strong localization at one lattice site only. In contrast, under an appropriate inclusion of correlation effects, it is seen that energy is gained in an ideal BT crystal if the electron is delocalized from a single Ti^{3+} site at least onto its first Ti neighbors and even beyond. The calculation predicts that 28% of the conduction-electron density is found at the central Ti site, 44% is transferred to the four nearest Ti sites along [100]-type directions, and 28% to the four next-nearest Ti positions (along [110]-type directions). For visualization of this extent of the electron density, see Figs. 10 and 13. It was also found that electron density is almost entirely restricted to one [100]-type plane. This proves the presence of a JT effect also in the case of such an intermediate polaron theoretically: the energy would be higher if the electron was delocalized also into the equivalent [010] and [001] planes. So the local cubic symmetry is broken. However, the studies also show that the intermediate polaron is not only stabilized by coupling to an *e*-type JT-vibration mode but also to an *a*-type breathing mode. This is expected because of the charge unbalance of Ti^{3+}: The Coulomb field originating from this extra charge is nearly isotropic in the nearly cubic crystal, inducing a breathing ionic screening and corresponding binding. A total-energy gain of 2.15 eV by coupling of the electron to the lattice was identified; this is the sum of the JT energy, 0.09 eV, and the breathing contributions, 2.06 eV. In order to find the net stabilization energy the 2.15 eV would have to be subtracted from half the conduction bandwidth. The low-energy subpeak[44] of the $BaTiO_3$ conduction band has a half-width of about 2 eV,[45] indicating that the polaron level will lie close to the rigid-lattice conduction-band edge. The estimate thus shows that a Ti^{3+} electron is on the verge of forming small polarons. Experimentally, the JT coupling is more directly

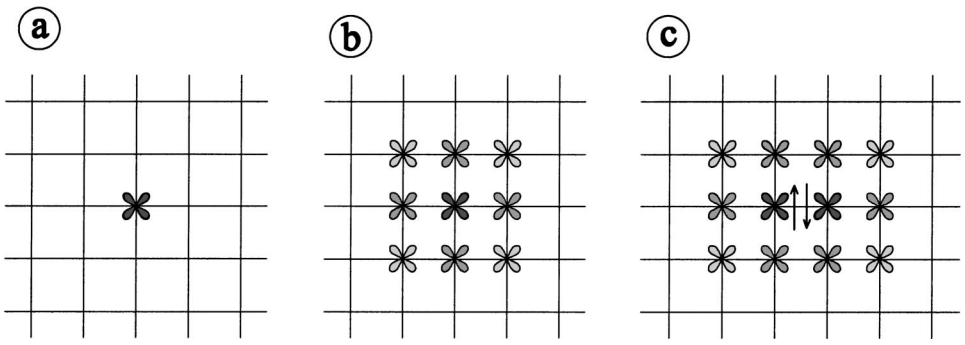

FIG. 13. (a) Schematical indication of the Ti^{3+} electron density of a small polaron, (b) electron density of the intermediate polaron eigenstate of ideal $BaTiO_3$, as based on Ref. 29, and (c) assumed electron-density distribution of Ti^{3+} bipolarons in $BaTiO_3$, as based on (b).

available, because it alone breaks the point symmetry and thus causes the anisotropy of the g tensor. From $g_\perp$ [Eq. (2)] one calculates

$$E_{\mathrm{JT}}=\frac{2}{3}\frac{2k\lambda}{g_e-g_\perp}. \tag{5}$$

For the investigated paramagnetic Ti^{3+} objects and for Mo^{5+} one derives the JT energies E_{JT}: Ti^{3+} small polaron: 0.072 eV, Ti^{3+} intermediate polaron: 0.060 eV, and Mo^{5+} JT ion: 0.233 eV, using the values $\lambda(Ti^{3+})=154\ \mathrm{cm}^{-1}$, $\lambda(Mo^{5+})=1030\ \mathrm{cm}^{-1}$, and, as an estimate, $k=0.8$. It is seen that the empirical JT coupling energies for Ti^{3+} are close to those predicted theoretically.

VIII. SUMMARY

By EPR investigations of very pure $BaTiO_3$, containing about 100 ppm Nb as extrinsic defects, at temperatures between 4.2 and 20 K and employing uniaxial stresses between 0 and 0.26 GPa, we identified two paramagnetic manifestations of Ti^{3+} $(3d^1)$ conduction polarons. Ti^{3+} compensates the Nb^{5+} impurities and is not, in most cases, associated with Nb^{5+}, which thus apparently represents a rather shallow donor potential. The first Ti^{3+} species has a relatively localized wave function and is therefore considered to be a small polaron. It has axial symmetry with an axis easily reorientable along the direction of uniaxial stress. This indicates first that Ti^{3+} is isolated and second that the axial symmetry is caused by a JT effect, $T_2\times e$. Both features show that two symmetries are broken: Ti^{3+} in an environment of equivalent Ti^{4+} ions breaks the translational symmetry of the crystal; the axial Jahn-Teller distortion indicates that the essentially cubic site symmetry is also broken. For comparison the Jahn-Teller effect of the extrinsic ion Mo^{5+}. $(4d^1)$ was also investigated. Consistent with the Jahn-Teller distortion it exhibits the same reorientation features as Ti^{3+}. In addition the latter ion shows a shift of its g value, indicating that the Jahn-Teller coupling is changed under stress. This is absent for Mo^{5+}. The reason for this change must thus be sought in the tendency of the Ti^{3+} orbital to delocalize, expected because of its equivalent Ti neighbors. A larger orbital has a lower Jahn-Teller coupling. This is proved by calculating the phonon form factor of the system for varying orbital radii. The Ti^{3+} orbital will expand if the electron can tunnel freely. Uniaxial stress apparently removes obstacles impeding tunneling. We think that these consist of strain fluctuations caused by the superposition of the local Jahn-Teller distortions. Under uniaxial stress the distortions are aligned and the crystal becomes more homogeneous, allowing a less restricted tunneling.

In this way the previous small polarons turn over to those of intermediate size and merge with the larger reservoir of such objects present already before applying stress. They probably exist in crystal regions that are already less strained before applying stress. A theoretical modeling of electron polarons in BT by embedded-cluster calculations indicates that the intermediate polarons are the eigenstates of an unperturbed crystal. Polarons of this type are also paramagnetic and can be aligned under uniaxial stress, indicating that they likewise owe their axiality to a JT effect. Their alignment behavior, however, is different from that of the small polarons. These turn the plane of their ground-state orbitals perpendicular to the stress axis, whereas for the intermediate ones the orbital planes are parallel to the stress axis. This different behavior is attributed to the fact that the small polarons are stabilized by local stress-induced distortions supporting the Jahn-Teller effect, whereas the intermediate polarons are favored by orbital orientations enhancing tunneling. Numerous further observations corroborate this model, such as decrease of the intermediate polaron linewidth under stress and its rise under growing temperature.

The concentration of polarons rises exponentially with increasing temperature. Apparently they originate from a diagmagnetic background reservoir, representing the third manifestation of Ti^{4+} polarons. Their diamagnetism is consistent with the assumption that they represent bipolarons, i.e., two electrons at neighboring Ti^{3+} sites, attracting each other by joint lattice distortion, which overcompensates their Coulomb repulsion. The binding energy of these electron pairs is rather small, about 10 meV. The presence of bipolarons requires that these should be present in the low-temperature ground-state of the crystal. The observation of paramagnetic Ti^{3+} objects then apparently is based on a metastable situation: They represent those few electrons kinetically hindered from diffusion-limited recombination to bipolarons.

Also Ti^{3+} polarons bound to defects created by reducing BT have been identified. They show g values similar to those of the free polarons discussed before. Assessment of all experimental facts indicates that they are bound to oxygen vacancies filled with two diamagnetically paired electrons.

ACKNOWLEDGMENTS

We thank D. Emin for illuminating discussions and V. G. Vikhnin for fruitful cooperation during the initial stages of this work. The investigations were supported by the DFG, Sonderforschungsbereich 225.

[1] P. Gerthsen, R. Groth, K. H. Härdtl, D. Heese, and H. G. Reik, Solid State Commun. **3**, 165 (1965).
[2] H. G. Reik and D. Heese, Phys. Solid State **24**, 281 (1967).
[3] E. V. Bursian, Y. G. Girshberg, Y. A. Grushevsky, and V. V. Shapkin, Ferroelectrics **8**, 417 (1974).
[4] A. Feltz and H. Langbein, Ferroelectrics **15**, 7 (1977).
[5] H. Ihrig and D. Hennings, Phys. Rev. B **17**, 4592 (1978).
[6] J. P. Boyeaux and F. M. Michel-Calendini, J. Phys. C **12**, 545 (1979).
[7] O. F. Schirmer, in *Defects and Surface Induced Effects in Advanced Perovskites*, edited by G. Borstel (Kluwer, Dordrecht, 2000), p. 75.

[8] S. Köhne-Lenjer, O. F. Schirmer, H. Hesse, T. W. Kool, and V. Vikhnin, J. Supercond. **12**, 193 (1999).
[9] D. Emin and T. Holstein, Phys. Rev. Lett. **36**, 323 (1976).
[10] J. T. Devreese, Encyclopedia of Applied Physics **14**, 383 (1996).
[11] A. L. Shluger and A. M. Stoneham, J. Phys.: Condens. Matter **5**, 3049 (1993).
[12] F. S. Ham, *Electron Paramagnetic Resonance*, edited by S. Geschwind (Plenum New York, 1972), Chap. 1.
[13] R. W. Reynolds and L. A. Boatner, Phys. Rev. B **12**, 4735 (1975).
[14] K. H. Höck, H. Nickisch, and H. Thomas, Helv. Phys. Acta **56**, 237 (1983).
[15] J. G. Bednorz and K. A. Müller, Rev. Mod. Phys. **60**, 585 (1988).
[16] K. A. Müller, J. Supercond. **15**, 863 (2000).
[17] K. A. Müller, Physica C **341–348**, 11 (2000).
[18] P. B. Allen and V. Perebeinos, Phys. Rev. Lett. **83**, 4828 (1999).
[19] B. Hellermann, F. Baller, B. Gather, H. Hesse, and R. Pankrath, Ferroelectrics **124**, 67 (1991).
[20] E. Possenriede, H. Kröse, T. Varnhorst, R. Scharfschwerdt, and O. F. Schirmer, Ferroelectrics **151**, 199 (1994).
[21] T. W. Kool, Ph.D. thesis, University of Amsterdam, 1991.
[22] R. N. Schwartz, B. A. Wechsler, and L. West, Appl. Phys. Lett. **67**, 1352 (1995).
[23] A. Hackmann and O. Kanert, Radiat. Eff. Defects Solids **119**, 651 (1991).
[24] T. Mitsui and S. Nomura, in *Ferroelektrika und Verwandte Substanzen*, edited by K. H. Hellwege and A. M. Hellwege, Landolt-Börnstein, New Series, Group III, Vol. 16 (Springer-Verlag, Berlin, 1981).
[25] O. F. Schirmer and D. von der Linde, Appl. Phys. Lett. **33**, 35 (1978).
[26] E. Patiño, F. Erazo, and A. Stashans, Mater. Lett. **50**, 337 (2001).
[27] A. Abragam and B. Bleaney, *Electron Paramagnetic Resonance of Transition Ions* (Clarendon, Oxford, 1970).
[28] G. D. Watkins and F. S. Ham, Phys. Rev. B **1**, 4071 (1970).
[29] A. Birkholz, Ph.D. thesis, University of Osnabrück, 1999.
[30] H. P. R. Frederikse, W. R. Hosler, W. R. Thurber, J. Babiskin, and P. G. Siebenmann, Phys. Rev. **158**, 775 (1967).
[31] B. W. Faughnan, Phys. Rev. B **5**, 4925 (1972).
[32] B. Y. Moizhes and S. G. Suprun, Fiz. Tverd. Tela (Leningrad) **26**, 896 (1984) [Sov. Phys. Solid State **26**, 544 (1984)].
[33] B. K. Chakraverty and C. Schlenker, J. Phys. C **37**, 353 (1976).
[34] K. P. O'Donnell, K. M. Lee, and G. D. Watkins, Physica B & C **116**, 258 (1983).
[35] R. Scharfschwerdt, A. Mazur, O. F. Schirmer, H. Hesse, and S. Mendricks, Phys. Rev. B **54**, 15 284 (1996).
[36] M. O. Selme and P. Pecheur, J. Phys. C **16**, 2559 (1983).
[37] S. A. Prosandeyev and I. A. Osipenko, Phys. Status Solidi B **192**, 37 (1995).
[38] H. Donnerberg and A. Birkholz, J. Phys.: Condens. Matter **12**, 8239 (2000).
[39] C. H. Park and D. J. Chadi, Phys. Rev. B **57**, 13 961 (1997).
[40] N. E. Christensen, E. A. Kotomin, R. I. Eglitis, A. V. Postnikov, G. Borstel, D. L. Novikov, S. Tinte, M. G. Stachiotti, and C. O. Rodriguez, in *Defects and Surface Induced Effects in Advanced Perovskites* (Ref. 7), p. 3.
[41] K. A. Müller, W. Berlinger, and R. S. Rubins, Phys. Rev. **186**, 361 (1969).
[42] G. D. Watkins, Adv. Solid State Phys. **24**, 163 (1984).
[43] D. M. Smyth, *The Defect Chemistry of Metal Oxides* (Oxford University, New York, 2000).
[44] L. Kantorowich, A. Stashans, E. Kotomin, and P. W. W. Jacobs, Int. J. Quantum Chem. **52**, 1177 (1994).
[45] M. Cardona, Phys. Rev. **140**, A6515 (1965).